Adsorption (2006) 12:103–117
DOI 10.1007/s10450-006-0373-3

Removal and recovery of vanadium(V) by adsorption onto $ZnCl_2$ activated carbon: Kinetics and isotherms

C. Namasivayam · D. Sangeetha

Received: 19 June 2005 / Revised: 5 July 2006 / Accepted: 10 July 2006

Abstract Adsorption of vanadium(V) from aqueous solution onto $ZnCl_2$ activated carbon developed from coconut coir pith was investigated to assess the possible use of this adsorbent. The influence of various parameters such as agitation time, vanadium concentration, adsorbent dose, pH and temperature has been studied. First, second order, Elovich and Bangham's models were used to study the adsorption kinetics. The adsorption system follows second order and Bangham's kinetic models. Langmuir, Freundlich, Dubinin-Radushkevich and Temkin isotherms have been employed to analyze the adsorption equilibrium data. Equilibrium adsorption data followed all the four isotherms—Langmuir, Freundlich, D-R and Temkin. The Langmuir adsorption capacity (Q_0) was found to be 24.9 mg g^{-1} of the adsorbent. The per cent adsorption was maximum in the pH range 4.0–9.0. The pH effect and desorption studies showed that ion exchange mechanism might be involved in the adsorption process. Thermodynamic parameters such as ΔG^0, ΔH^0 and ΔS^0 for the adsorption were evaluated. Effect of competitive anions in the aqueous solution such as PO_4^{3-}, SO_4^{2-}, ClO_4^-, MoO_4^{2-}, SeO_3^{2-}, NO_3^- and Cl^- was examined. SEM and FTIR were used to study the surface of vanadium(V) loaded $ZnCl_2$ activated carbon. Removal of vanadium(V) from synthetic ground water was also tested. Results show that $ZnCl_2$ activated coir pith carbon is effective for the removal of vanadium(V) from water.

Keywords Adsorption · Activated carbon · Vanadium(V) · Kinetics · Isotherms · pH · Foreign ions

C. Namasivayam (✉) · D. Sangeetha
Environmental Chemistry Division, Department of Environmental Sciences,
Bharathiar University, Coimbatore-641 046, India
e-mail: cnamasi@yahoo.com

Introduction

Vanadium compounds have harmful effects on the circulatory system and disturb the metabolism including that of plants, as they cause chlorosis and limit growth (Kabata-Pendias and Pendias, 1993). Vanadium compounds have been found to lower the elevated food glucose, cholesterol and triglycerides in diabetic rats (Cater and Quintus, 1979). Contamination of vanadium compounds in wastewater remains a major water pollution problem. Furthermore, vanadium concentration in natural waters has been reported from 29.5 to 37.4 nmol dm^{-3} (Prange and Kremling, 1985). Bureau of Indian Standards (1981) have set a limit of 0.2 mg dm^{-3} vanadium in surface water.

Vanadium compounds are of particular interest in many application areas. Wastes from industrial areas can have more vanadium due to the anthropogenic activities such as emission by petroleum refineries, metal plants and phosphorite treating factories (Kabata-Pendias and Pendias, 1993) and also a component of alkaline and argillaceous rocks (Kabata-Pendias

and Pendias, 1979). Moreover vanadium compounds are found in phosphorous ores, many foods, particularly fats and oils. Vanadium is also present in significant concentrations in fuel oil (Guzman et al., 2002); its combustion in thermal power plants leads to the production of toxic fly ash. Vanadium/ phosphoric acid system is used as corrosion inhibitor in the place of Cr(VI) in steel industries (Blackmore, 1996). These wastes cannot be disposed of directly into the environment since vanadate can be easily leached by rainwater (Guzman et al., 2002).

Water pollution by vanadium is not only a public health concern, but an economic one as well. Therefore removal of this ion from wastewaters and ground waters is of significant importance from an environmental point of view (Abbas and Conway, 2002). Vanadium concentrations are not high enough to make their extraction by standard processes for the treatment of dilute solutions. Biological and chemical treatments (Kunz, 1976) are applied to remove this trace element. Recently, interest has been focused on materials of biological origins: namely byproducts from agriculture and biopolymers (Guzman et al., 2002; Guibal et al., 1998). Chemical methods include adsorption/coprecipitation on iron oxyhydroxide (Blackmore, 1996). Adsorption of V(IV) on chitosan (Jansson-Charrier, 1996), high area carbon cloth (Abbas and Conway, 2002) and commercial crystalline calcium hydroxyapatite (Vega, 2003) has been reported.

Coir pith is an agricultural solid waste indigenously available in coconut fibre industries. It is a light fluffy material, which is generated in the separation process of the fiber from coconut husk. Annual production of coir pith is around 7.5 million tons (Gopal and Gupta, 2001). Coir pith accumulation around coir fiber industries is creating a menace. This abundant raw coir pith consists of 27.1% of cellulose, 28.3% of lignin and 8.1% of soluble tannin like phenolic compounds (Vinodhini et al., 2005). Lignocellosic waste was used to develop $ZnCl_2$ activated carbon and applied to the removal of phosphate from water (Namasivayam and Sangeetha, 2004).

The objective of this work was to evaluate the potential of $ZnCl_2$ activated coir pith carbon for the adsorption of vanadium(V). Adsorption dynamics, equilibrium studies and effects of pH, adsorbent dose and temperature were studied. The per cent removal of V(V) in the presence of varying concentration of foreign anions was examined. Application to treatment of synthetic ground waters containing V(V) was also carried out.

Experimental procedure

Material and methods

Coir pith was collected from local coir industries. It was dried in sunlight for 5 h and then $ZnCl_2$ activated coir pith carbon was prepared. Coir pith was stirred into a boiling solution containing $ZnCl_2$ in the weight ratio of 2:1. The filtered material was washed, dried and carbonized at 700°C under controlled conditions. After cooling, the excess zinc chloride present in the carbonized material was leached out using dilute HCl. Then the carbon was repeatedly washed with water to get rid of traces of HCl and $ZnCl_2$. This was ascertained by analyzing the wash water each time using silver nitrate (Namasivayam and Sangeetha, 2004). The carbonized material was sieved to 250 to 500 μm size and characterized using physico-chemical methods and used for adsorption studies.

Specific surface area and pore size distribution were determined from nitrogen adsorption/desorption isotherms measured at 77 K by an AUTOSORB 1-MP (Quantachrome, Boynton Beach, FL, USA) Computer controlled Surface Area Analyzer. All isotherms consisted of 40 adsorption and 19 desorption points. The total pore volume was calculated at a P/Po-value of approx. 0.95, which corresponds to a pore diameter of approx 2.06 nm i.e. all pores up to this diameter were completely filled with N_2. Surface functional groups and other parameters were determined using standard methods (APHA, 1992; ASTM, 1999). Surface functional groups were determined by using Boehm's titration. Carbon was mixed with 0.1 M solution of NaOH, Na_2CO_3, $NaHCO_3$ or HCl. The number of basic sites was calculated from the amount of HCl that reacted with the carbon. The various free acidic groups were determined using the assumption that NaOH neutralizes carboxyl, lactone and phenolic groups; Na_2CO_3 neutralizes carboxyl, lactone; $NaHCO_3$ neutralizes only carboxyl groups, respectively (Laszlo and Szucs, 2001). Fourier Transform Infrared (FTIR) Spectra were obtained using Shimadzu, Model FTIR - 8201PC. The transmission spectra of the samples were recorded using KBr wafers. Morphological features of samples were obtained with a Hitachi 2300 Scanning Electron Microscope.

Vanadium(V) solutions were prepared from ammonium vanadate, obtained from s.d. Fine Chemicals, Mumbai, India. Solutions of nitrate, sulfate, chloride,

selenite, perchlorate and molybdate were prepared from their sodium salts and phosphate from its potassium salt. Synthetic ground waters containing 20 and 40 mg dm^{-3} V(V) were prepared and the composition is chloride, 63.6 mg dm^{-3}; sulfate, 55.1 mg dm^{-3}; nitrate, 36.5 mg dm^{-3}, phosphate, 34.9 mg dm^{-3}; sodium, 56.9 mg dm^{-3}; calcium 36.4 mg dm^{-3}; potassium, 59.3 mg dm^{-3}.

Adsorption studies

Adsorption experiments were carried out by agitating 200 mg of adsorbent with 50 cm^3 of V(V) solution of desired concentration and pH at 200 rpm, 35°C in a thermostated rotary shaker (ORBITEK, Chennai, India). At the end of the predetermined time intervals, the samples were taken out and the supernatant solution was centrifuged at 10,000 rpm for 20 min. Then the centrifugate was analyzed for the residual V(V) by colorimetric method (Jansson-Charrier et al., 1996) on a UV-Visible spectrophotometer (Hitachi, Model U-3210, Tokyo). Effect of pH was studied in the pH range 2.0 to 11.0 by adjusting the pH of V(V) solutions using dilute HCl and NaOH solutions by means of a pH meter (Elico, Mode LI-107, Hyderabad, India). Effect of adsorbent dose was studied by agitating 50 cm^3 of 20, 40, 60, 80 or 100 mg dm^{-3} V(V) solutions with different adsorbent doses (50–400 mg) at time intervals longer than the equilibrium time.

Desorption studies

The adsorbent (200 mg/50 cm^3) that was used for the adsorption of 20, 40, 60 or 80 mg dm^{-3} of V(V) solution was separated from the solution by sedimentation. The V(V) loaded adsorbent was suction-filtered using Whatman filter paper and washed gently with water to remove any unadsorbed V(V). Several such samples were prepared. Then the spent adsorbent was mixed with 50 cm^3 of distilled water samples at pH values in the range 2.0 to 12.0, adjusted using dilute HCl/NaOH and agitated at time intervals longer than the equilibrium time. The desorbed V(V) was estimated as before.

Temperature study

Effect of temperature was studied using 40, 60, 80, 100 and 120 mg dm^{-3} of V(V) and 200 mg of adsorbent at 35, 40, 50 and 60°C in the thermostated rotary shaker.

Preliminary experiments showed that there was no adsorption due to container walls. Experiments were carried out in duplicate and mean values were taken for calculations. Maximum deviation was 3%.

Results and discussion

Characteristics of coir pith carbons

The characteristics of $ZnCl_2$ activated coir pith carbon in comparison with coir pith carbon in the absence of $ZnCl_2$ activation are presented in Table 1. Most of the surface (90%) and pore volume (75%) is made up by pores smaller than 2 nm in pore width, the so called micropores. The carbon has a sponge like structure, due to the very high value of the fractal dimension with 2.93. Activation with $ZnCl_2$ in coir pith generates more interspaces between carbon layers leading to more microporosity and more surface area compared to the carbon prepared in the absence of $ZnCl_2$ (167 m^2g^{-1}) (Namasivayam and Kavitha, 2003). One of the most important roles played by $ZnCl_2$ includes causing electrolytic action, termed as "swelling" in the molecular structure of cellulose which is the chief material in any carbonaceous starting material. Swelling caused by action of $ZnCl_2$ in breaking of the lateral bonds in the cellulose molecules results in increased "inter" and "intra" miscelle voids. As a result, $ZnCl_2$ promotes the development of porous structure of the activated carbon because of the formation of small elementary crystallites (Smisek and Cerney, 1970; Sabio and Reinoso, 2004). The pore size distribution supports the above statements. The acidic surface functional groups present on the carbon are: carboxylic, 0.282 meq g^{-1}(19.4%); lactones, 0.234 meq g^{-1} (16.1%); phenolic, 0.90 meq g^{-1} (64.6%) and basic groups, 0.77 meq g^{-1}. The Scanning Electron Microscopy (SEM) pictures of the carbon before(a) and after adsorption(b) of V(V) are shown in Fig. 1. The SEM photograph of $ZnCl_2$ activated carbon shows a large number of pores (Fig. 1(a)). But after adsorption the pores are filled by V(V) ions (Fig. 1(b)).

IR analysis permits spectrophotometric observation of the adsorbent surface in the range 400–4000 cm^{-1}, and serves as a direct means for the identification of the specific functional groups on the surface (Fig. 2). IR spectrum of the $ZnCl_2$ activated carbon before adsorption of V(V) shows peaks at 3400 cm^{-1}, 2922

Table 1 Characteristics of activated coir pith carbons

Parameter	Presence of $ZnCl_2$	Absence of $ZnCl_2$
Specific surface area ($m^2\ g^{-1}$)	910	167
Total pore volume ($cm^3\ g^{-1}$)	0.363	0.122
Micropore area ($m^2\ g^{-1}$)	284.0	89.3
Micropore volume ($cm^3\ g^{-1}$)	0.131	0.091
Average pore diameter (nm)	1.60	2.75
Average micropore diameter (nm)	0.90	1.20
pH_{ZPC}	3.20	8.00
pH (1% solution)	3.27	10.10
Conductivity (1% solution) (mS/cm)	0.26	2.30
Bulk density ($g\ cm^{-3}$)	0.10	0.12
Mechanical Moisture content (%)	12.67	5.88
Ash content (%)	3.20	8.00
Specific gravity	1.29	1.74
Porosity (%)	92.12	93.11
Volatile matter (%)	19.25	58.38
Fixed carbon (%)	81.73	41.62
Decolorizing power ($mg\ g^{-1}$)	137.00	21.00
Iodine number ($mg\ g^{-1}$)	203.04	101.52
Phenol number ($mg\ g^{-1}$)	30.00	–
Ion exchange capacity ($meq\ g^{-1}$)	0.11	Nil
Zinc (%)	0.02	–
Zinc leached (%)	0.01	–
Ash analysis:		
Sodium (%)	0.09	0.14
Potassium (%)	0.10	0.18
Calcium (%)	0.78	0.22
Phosphorous (%)	0.01	0.01

cm^{-1}, 2855 cm^{-1}, 2359 cm^{-1}, 1580 cm^{-1}, 1153 cm^{-1} and 675 cm^{-1}. Peak at 3400 cm^{-1} is assigned to OH stretching vibration. Bands at 2922 and 2855 cm^{-1} are ascribed to symmetric and asymmetric C–H stretching vibrations. Peak at 2359 cm^{-1} corresponds to strong O = C = O stretching vibrations. Asymmetric COO– vibration occurred at 1580 cm^{-1}. The 1153 cm^{-1} band may have contributions from both C=O stretching and O–H bending modes in phenolic groups (Jiang et al., 2003). The peak at 675 cm^{-1} can be ascribed to CH=Cl stretching vibration and/or to skeletal vibrations corresponding to hydrocarbons (Bellamy, 1975).

Spectral changes in the spectra of the unloaded (Fig. 2(a)) and loaded adsorbent (Fig. 2(b)) are on the basis of the changes in the nature of the surface like participation of specific functional groups in adsorption interaction and the ensuing chemical changes thereon. Vanadium(V) loaded carbon has slightly shifted 3400 cm^{-1} peak (strong) corresponding to OH stretching vibration to 3429 cm^{-1} and reduced the absorption of the strong peak at 2360 cm^{-1} corresponding to O = C = O stretching vibration and 1580 cm^{-1} corresponding COO– vibration. There are two new peaks (weak) at 1455 cm^{-1} and 471 cm^{-1}.

Effect of agitation time and initial vanadium(V) concentration

Amount of V(V) adsorption increased with time and reached equilibrium at 30, 30, 40, 40 and 40 min for 40, 60, 80, 100 and 120 mg dm^{-3} of V(V) (Fig. 3). The equilibrium time and the uptake of V(V) are dependent of initial concentration of adsorbate. The amount of V(V) adsorbed, q ($mg\ g^{-1}$), increased with increase in V(V) concentration and remained nearly constant after equilibrium time. It shows that the adsorption at different concentrations was rapid in the initial stages and gradually decreased with the progress of adsorption until the equilibrium reached. The curves also indicate that the adsorption led to saturation, suggesting the possible

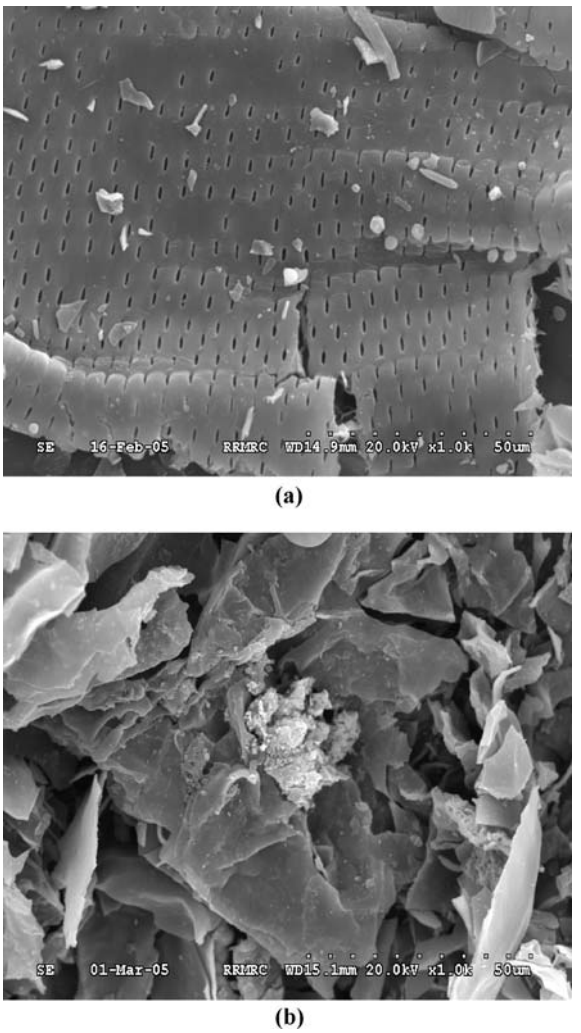

Fig. 1 SEM photographs of the $ZnCl_2$ activated carbon before (a) and after adsorption of V(V) (b)

monolayer coverage of V(V) on the surface of the adsorbent. The vanadium(V) removal decreased from 87 to 65% as the V(V) concentration was increased from 40 to 120 mg dm^{-3} and the amount of V(V) adsorbed increased from 8.7 to 19.4 mg g^{-1}.

Adsorption kinetics

Adsorption kinetics model correlates the adsorbate uptake rate with the bulk concentration of the adsorbate; these models are important in water/wastewater treatment process design and optimization.

In order to investigate the mechanism of adsorption and rate controlling steps, the kinetic data were modeled using Lagergren first order, second order and Elovich equations.

(a) *First order kinetic model*

Lagergren (1898) suggested a first order equation for the sorption of liquid/solid system based on solid capacity. The Lagergren rate equation is the most widely used adsorption rate equation for the adsorption of adsorbate from aqueous solution. The Lagergren first order model can be represented as:

$$dq/dt = k_1 (q_e - q) \tag{1}$$

Integrating Eq. (1) for the boundary conditions $t = 0$ to $t = t$ and $q = 0$ to $q = q$, gives

$$\log (q_e - q) = \log q_e - k_1 t/2.303 \tag{2}$$

where q_e and q are the amounts of V(V) adsorbed (mg g^{-1}) at equilibrium and at time t, respectively, and k_1 is the rate constant of first order adsorption (min^{-1}). Values of q_e and k_1 were calculated from the slope and intercept of the plot of log ($q_e - q$) *vs* t (Figure not shown).

(b) *Second order kinetic model*

The second order kinetic model is represented as (Ho and McKay, 1998):

$$dq_t/dt = k_2 (q_e - q_t)^2 \tag{3}$$

Integrating Eq. (3) for the boundary conditions $t = 0$ to $t = t$ and $q_t = 0$ to $q_t = q$, gives

$$1/(q_e - q) = 1/q_e + k_2 t \tag{4}$$

where k_2 is the rate constant of second order adsorption (g mg^{-1} min^{-1}). Equation (4) can be rearranged to obtain a linear form:

$$t/q = 1/k_2 q_e^2 + t/q_e \tag{5}$$

where k_2 is the equilibrium rate constant of second order adsorption (g $mg^{-1}min^{-1}$). Values of k_2 and q_e were calculated from the slope and intercept of the plots t/q *vs* t (Fig. 4 and Table 2).

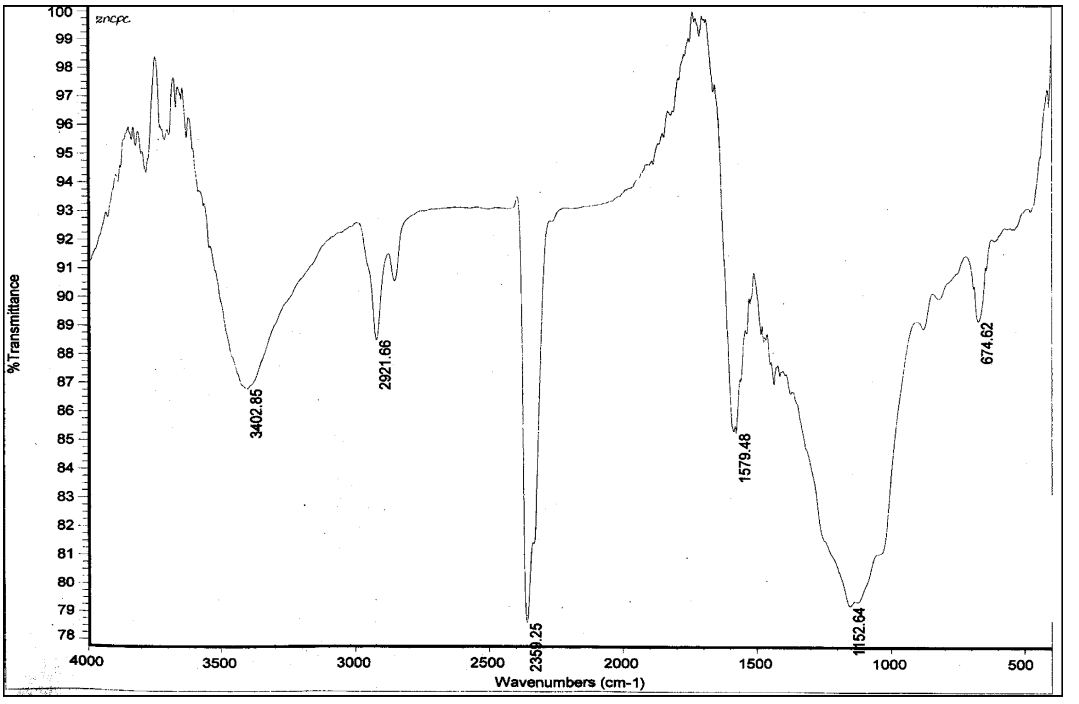

(a)

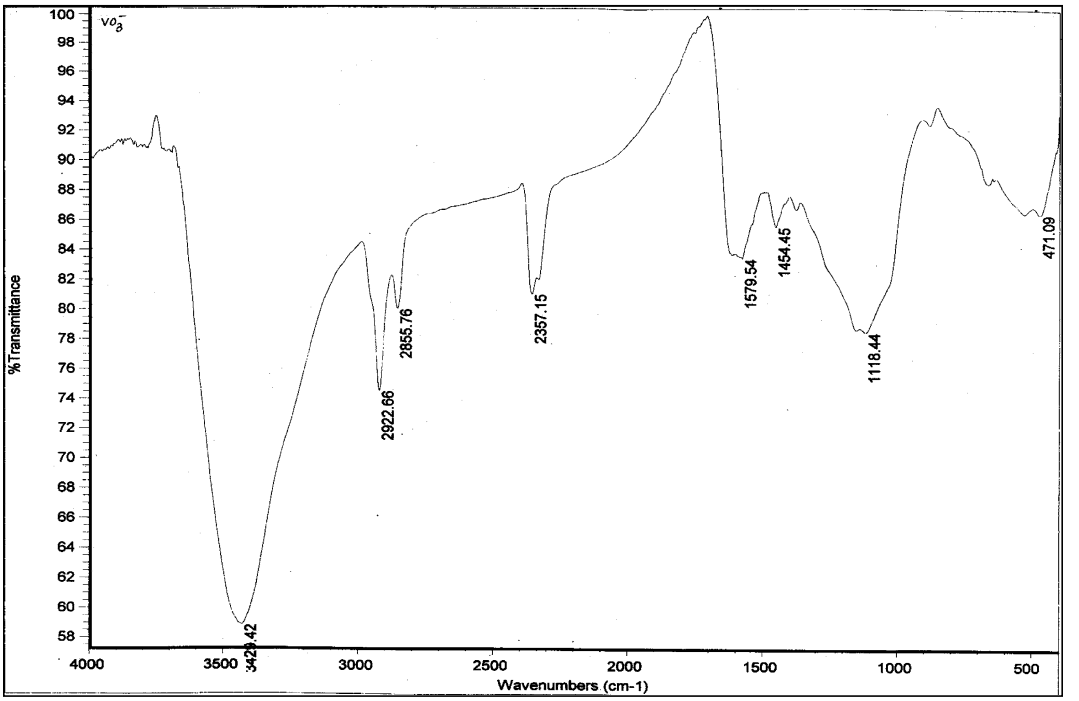

(b)

Fig. 2 FTIR spectrum of the $ZnCl_2$ activated carbon before (a) and after adsorption of V(V) (b)

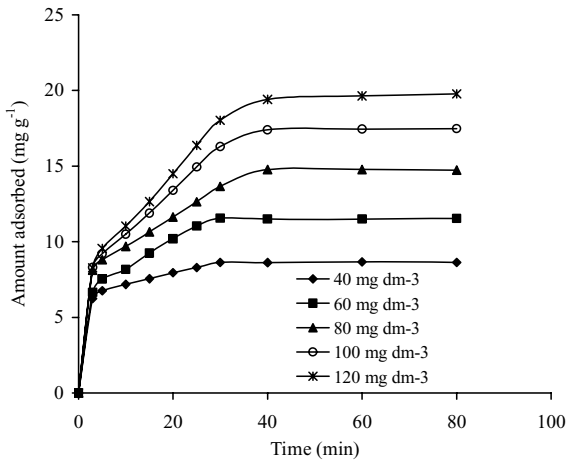

Fig. 3 Effect of agitation time and concentration of V(V) on removal: Adsorbent dose, 200 mg/50 cm^3; pH, 4.0; Temp, 35°C

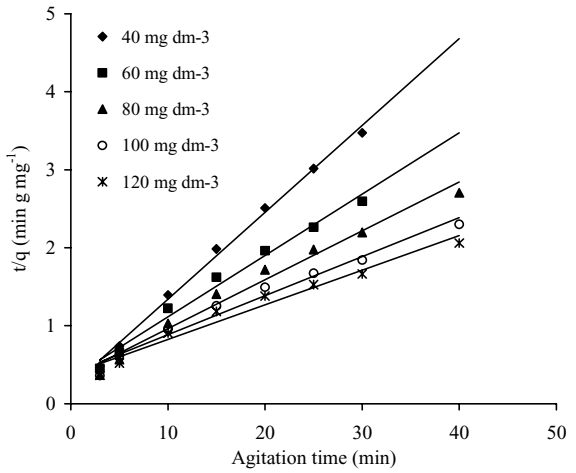

Fig. 4 Plots of the pseudo second-order model at different initial V(V) concentrations: Adsorbent dose, 200 mg/50 cm^3, pH, 4.0; Temp, 35°C

(c) *Elovich equation*

A widely used equation to describe the kinetics of chemisorption of gas on solids was proposed by Elovich (Cheung et al., 2000). The Elovich equation was derived from the Elovich kinetic equation:

$$dq/dt = \alpha e^{-\beta q} \tag{6}$$

Integrating the rate equation with the boundary conditions $t = 0$ to $t = t$ and $q = 0$ to $q = q$, gives

$$q = (1/\beta)\ln(\alpha\beta) + (1/\beta)\ln(t + t_0) \tag{7}$$

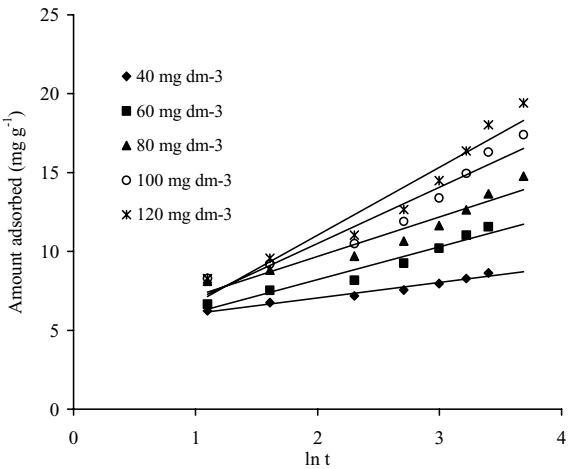

Fig. 5 Plots of the Elovich kinetic model at different initial V(V) concentrations: Adsorbent dose, 200 mg/50 cm^3, pH, 4.0; Temp, 35°C

where α and β are the parameters of the equation and $t_0 = 1/(\alpha\beta)$; α represents the rate of chemisorption at zero coverage (mg g^{-1} min^{-1}) and β is related to the extent of surface coverage and activation energy for chemisorption (g mg^{-1}).

When $t_0 << t$, then Eq. (7) is replaced by

$$q = (1/\beta)\ln(\alpha\beta) + (1/\beta)\ln t \tag{8}$$

The constants, α and β, are calculated from the plots of q *vs* ln t (Fig. 5).

The results of fitting of kinetic data to the first and second order models (the experimental and calculated q_e values and calculated rate constants) and Elovich model are presented in Table 2. Values of q_e calculated from the first order model do not agree with the experimental q_e values. While q_e values calculated from the second order kinetic model are close to the experimental q_e values with good correlation coefficients. Hence the adsorption system follows second order kinetic model. Similar phenomenon has been observed in the adsorption of phosphate on calcined alunite (Mahmut, 2003) and $ZnCl_2$ activated coir pith carbon (Namasivayam and Sangeetha, 2004). The experimental data also fit well with the Elovich equation (Fig. 5). This suggests that the sorption system studied belong to the second order kinetic model based on the assumption that the rate determining step may be chemical sorption or chemisorption involving valence forces through sharing or exchange of electrons between adsorbent

Table 2 Comparison of first order and second order adsorption rate constants and calculated and experimental q_e values for different initial V(V) concentrations and Elovich kinetic model

		First order kinetic model			Second order kinetic model			Elovich kinetic model		
Parameter	q_e (exp) (mg g^{-1})	k_1 (min^{-1})	q_e (cal) (mg g^{-1})	R^2	k_2 (g $mg^{-1}min^{-1}$)	q_e (cal) (mg g^{-1})	R^2	α (mg g^{-1} min^{-1})	β (g mg^{-1})	R^2
Initial V(V) conc(mg dm^{-3})*										
40	8.6	0.081	3.1	0.9711	0.056	8.9	0.9980	175.7	1.019	0.9705
60	11.6	0.094	7.4	0.9294	0.020	12.7	0.9930	14.5	0.480	0.9486
80	14.8	0.061	8.9	0.9402	0.012	15.9	0.9900	16.1	0.399	0.9240
100	17.4	0.072	13.2	0.9238	0.007	19.9	0.9754	9.2	0.281	0.9315
120	19.5	0.071	15.9	0.9229	0.005	22.5	0.9657	7.5	0.232	0.9308
Temp (°C)+										
35	8.6	0.081	3.1	0.9711	0.056	8.9	0.9980	175.7	1.019	0.9705
40	8.9	0.112	3.2	0.9375	0.068	9.2	0.9970	349.3	1.048	0.9675
50	9.1	0.094	2.4	0.9822	0.085	9.4	0.9964	813.5	1.104	0.9522
60	9.5	0.150	2.5	0.9985	0.108	10.0	0.9989	1185.0	1.041	0.9903

*Conditions: Adsorbent dose, 200 mg/50 cm^3; pH 4.0; Temperature, 35°C.
+Conditions: V(V) conc., 40 mg dm^{-3}; Adsorbent dose, 200 mg/50 cm^3; pH 4.0.

and adsorbate (Cheung et al., 2000). Zeng et al. (2004) found that Elovich equation provide satisfactory fitting of the kinetic data of phosphate adsorption on the iron oxide tailings.

Effect of adsorbent dose

The removal of V(V) by $ZnCl_2$ activated coir pith carbon at different doses from 50−400 mg/50 cm^3 for V(V) concentration of 20 to 100 mg dm^{-3} was studied. It was found that increase in adsorbent dose increased the removal of V(V) and quantitative removal occurred at 250, 350, 400, 500 and 500 mg/50 cm^3 for 20, 40, 60, 80 and 100 mg dm^{-3} of V(V), respectively.

Adsorption isotherms

The equilibrium of a solute separated between liquid and solid phase is described by various models of adsorption isotherms such as the Langmuir (1918); Freundlich (1906), Dubinin-Radushkevich (Ozcan et al., 2005) and Temkin (Choy et al., 1999) models. Langmuir model suggests a monolayer adsorption, with no lateral interaction between the sorbed molecules. Freundlich model assumes heterogeneous adsorption due to the diversity of sorption sites or the diverse nature of the metal ions adsorbed, free or hydrolyzed species. Dubinin-Radushkevich does not assume an energetically homogeneous surface and proposes a nonhomogeneous distribution of adsorption sites. In particular, it assumes that ionic species bind first with the most energetically favorable sites and that multilayer adsorption then occurs. Temkin and Pyzhev (Choy et al., 1999) considered the effects of indirect adsorbate/adsorbate interactions on adsorption isotherms. According to the Temkin isotherm, the heat of adsorption of all the molecules in the layer would decrease linearly with coverage due to adsorbate/adsorbate interactions.

The Langmuir isotherm can be expressed as:

$$q_e = Q_0 b C_e/(1 + bC_e) \tag{9}$$

where q_e is the solid-phase adsorbate concentration at equilibrium (mg g^{-1}), C_e is the concentration of V(V) solution (mg dm^{-3}) at equilibrium. The constant Q_0 gives the theoretical monolayer adsorption capacity (mg g^{-1}) and b is related to the energy of adsorption (dm^3 mg^{-1}).

A linear expression for the Langmuir equation is expressed as:

$$C_e/q_e = 1/Q_0 b + C_e/Q_0 \tag{10}$$

Langmuir constants, Q_0 and b, were calculated from the linear plot of C_e/q_e *vs* C_e and found to be 24.9 mg g^{-1} and 0.077 $dm^3 mg^{-1}$, respectively (Table 3). The adsorption capacity of V(V) by coir pith carbon(in the absence of $ZnCl_2$) was found to be insignificant. The high surface area and micropore area of the $ZnCl_2$ activated carbon are responsible for the good adsorption capacity of the carbon for V(V). The Langmuir adsorption capacity Q_0 in the 2nd adsorption cycle was found to be 19.8 mg g^{-1} under the same experimental conditions as in the 1st adsorption cycle. Values of Q_0 and b for the adsorption of V(V) by chitosan (pH 4.0; rpm, 350; particle size, 250 to 500 μm) and chitosan beads (particle size, 250 to 500 μm) have been reported to be 420 mg g^{-1} and 0.216 dm^3 mg^{-1}; 146.8 mg g^{-1} and 0.21 dm^3 mg^{-1}, respectively (Guzman et al., 2002; Guibal et al., 1998). The high adsorption capacity of chitosan may be due to high protonation of the chitosan polymer.

The essential characteristics of the Langmuir isotherm can be expressed by a dimensionless constant called equilibrium parameter R_L (Hall et al., 1966).

$$R_L = 1/(1 + bC_0) \tag{11}$$

where b is the Langmuir constant and C_0 is the initial concentration (mg g^{-1}), R_L values indicate the type of isotherm. The R_L values between 0 and 1 indicate favorable adsorption. The R_L values were found to be between 0.098 and 0.248 for all the concentrations of V(V) studied.

The Freundlich isotherm model is expressed as:

$$q_e = k_f \log C_e^{1/n} \tag{12}$$

in logarithmic form,

$$\log q_e = \log k_f + 1/n \log C_e \tag{13}$$

where k_f is related to adsorption capacity and n is related to intensity of adsorption. The Freundlich constants, k_f and n were calculated from the linear plot

Table 3 Langmuir, Freundlich and Dubinin-Radushkevich constants

Langmuir			Freundlich			Dubinin-Radushkevich			Temkin		
Q_0 (mg g^{-1})	b (dm^3 mg^{-1})	R^2	k_f mg$^{1-1/n}$L$^{1/n}$g^{-1}	n	R^2	q_m (mg g^{-1})	β (mol^2 J^{-2})	R^2	B (mg g^{-1})	A (dm^3 mg^{-1})	R^2
24.90	0.08	0.9783	4.23	2.46	0.9880	5.36	0.80	0.9821	67.29	3.81x10^{-9}	0.9832

Conditions: Conc. of V(V), 40–120 mg dm^{-3}; Adsorbent dose, 200 mg/50 cm^3; pH 4.0; Temperature, 35°C.

of log q_e *vs* log C_e and are presented in Table 3. Values of k_f and n for the adsorption of V(V) by chitosan (pH 4.0; rpm, 350; particle size, 250 to 500 μm) and chitosan beads (particle size, 250 to 500 μm) were reported to be 120 and 3.36; 58.9 and 4.86, respectively (Guzman et al., 2002; Guibal et al., 1998).

The Dubinin-Radushkevich isotherm has the following form:

$$q_e = q_m e^{-B\varepsilon^2} \tag{14}$$

A linear form of Dubinin-Radushkevich (D-R) isotherm is:

$$\ln q_e = \ln q_m - B\varepsilon^2 \tag{15}$$

where q_m is the theoretical saturation capacity (mol g^{-1}), β is a constant related to the mean free energy of adsorption per mole of the adsorbate (mol^2 J^{-2}), and ε is the Polanyi potential which is related to the equilibrium concentration as follows:

$$\varepsilon = RT \ln(1 + 1/C_e) \tag{16}$$

where R is the universal gas constant (8.314 J mol^{-1} K^{-1}), C_e is the equilibrium concentration of adsorbate in solution (mol L^{-1}) and T(°K) is the absolute temperature. The D-R constants q_m and β were calculated from the linear plot of lnq_e *vs* ε^2 and are given in Table 3. The constant β gives an idea about the mean free energy E (kJ mol^{-1}) of adsorption per molecule of the adsorbate when it is transferred to the surface of the solid from infinity in the solution and can be calculated using the relationship:

$$E = 1/(2\beta)^{1/2} \tag{17}$$

This parameter gives information whether adsorption mechanism is ion-exchange or physical adsorption. If the magnitude of E is between 8 and 16 kJ mol^{-1}, the adsorption process follows by ion-exchange, while for the values of $E < 8$ kJ mol^{-1}, the adsorption process is of a physical nature (Ozcan et al., 2003). In the present study the numerical value of adsorption of the mean free energy is 11.46 kJ mol^{-1} which corresponds to ion-exchange process.

The Temkin isotherm is used in the form:

$$q_e = (RT/h) \ln(AC_e) \tag{18}$$

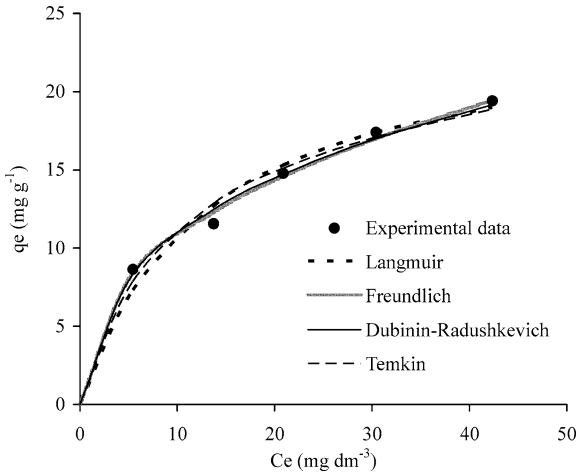

Fig. 6 Adsorption isotherms for adsorption of V(V)

The linear form of the Temkin isotherm can be expressed as:

$$q_e = B \ln A + B \ln C_e \tag{19}$$

where C_e is concentration of the anion at equilibrium (mol/L), q_e is the amount of anion adsorbed at equilibrium (mol/g), $RT/h = B$ and A and h are constants. The sorption data can be analyzed according to Eq. (19). Therefore, a plot of q_e *vs* $\ln C_e$ is used to determine the constants A and B.

Figure 6 presents different adsorption isotherms along with the experimental data. Correlation coefficients are shown in Table 3. In order to compare the validity of isotherm equations, a normalized deviation, $\Delta q(\%)$ was calculated using the following equation,

$$\Delta q\,(\%) = 100 \times \sqrt{\frac{\sum \left[\left(q_e^{\exp} - q_e^{cal}\right)/q_e^{\exp}\right]^2}{(n-1)}} \tag{20}$$

where superscripts 'exp' and 'cal' are the experimental and calculated values, respectively, and 'n' is the number of measurements (Wu et al., 2005). From the results, it was found that Δq obtained from Freundlich model is the lowest ($\Delta q(\%) = 3.61$) and it is a better fit than that of Langmuir ($\Delta q(\%) = 9.29$), D-R ($\Delta q(\%) = 4.47$) or Temkin ($\Delta q(\%) = 7.33$) adsorption isotherm models.

Effect of temperature

Increase of temperature slightly increased the per cent removal. Activation energy, Ea, was calculated using Arrhenius equation (Laidler and Meiser, 1999) and found to be 21.6, 29.1, 33.4, 47.5 and 52.3 kJ mol^{-1} for the V(V) concentrations of 40, 60, 80, 100 and 120 mg dm^{-3}, respectively (Fig. 7). Film diffusion typically has activation energy of 17–21 kJ mol^{-1} and pore diffusion has activation energy of 21–42 kJ mol^{-1} (Sparks, 1999). Thus the Ea values show that the adsorption of V(V) is pore-diffuison controlled.

The Gibb's free energy change is obtained using following relationship:

$$\Delta G^0 = -RT \ln b \tag{21}$$

where R is the gas constant and b is the Langmuir constant in dm^{3}mol^{-1} and T is the temperature in °K. Values of ΔG^0were found to be −21.18, −22.01, −23.36 and −25.38 kJ mol^{-1} at 35, 40, 50 and 60°C, respectively. The negative values of ΔG indicate the spontaneous nature of adsorption. Other thermodynamic parameters such as enthalpy and entropy are evaluated using van't Hoff equation:

$$\log b = \frac{\Delta S^0}{2.303R} - \frac{\Delta H^0}{2.303RT} \tag{22}$$

where ΔS^0 and ΔH^0 are changes in entropy and enthalpy of adsorption, respectively. The values of ΔH^0 and ΔS^0 were calculated from the slope and intercept of the van't Hoff linear plot of log b *vs* $1/T$ and found to be 29.7 kJ mol^{-1} and 164.9 J K^{-1} mol^{-1}, respectively.

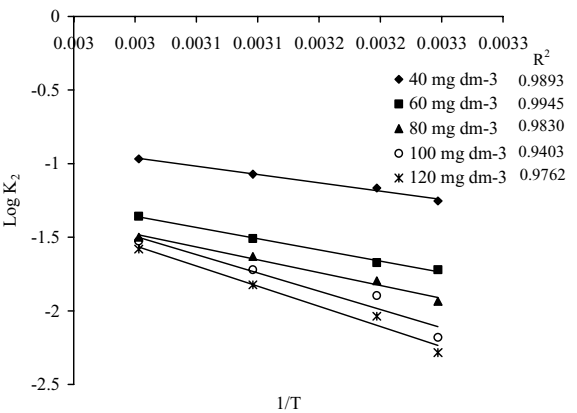

Fig. 7 Activation energy plots for adsorption of V(V)

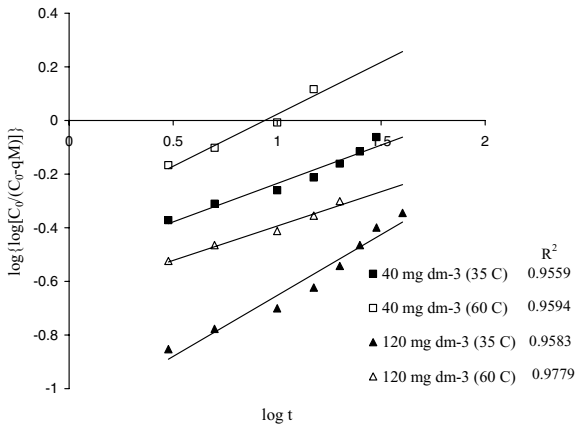

Fig. 8 Bangham's plots for adsorption of V(V)

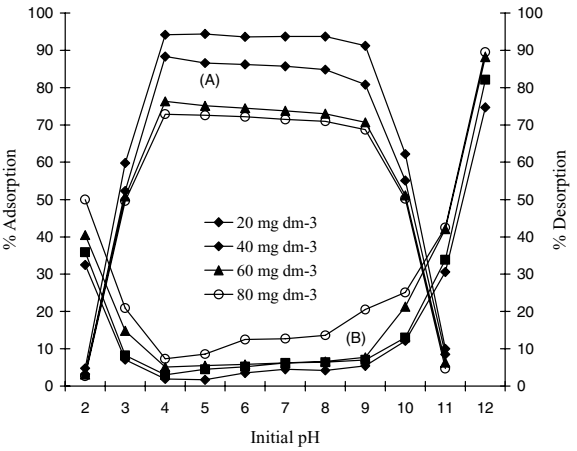

Fig. 9 Effect of pH on adsorption/desorption of V(V): Adsorbent dose 200 mg/50 cm^3; agitation time 45 min; Temp, 35°C

The positive value of ΔH^0 confirms the endothermic nature of adsorption. The enthalpy change (ΔH^0) for chemisorption is in the range, 40–120 kJ mol^{-1} (Alkan et al., 2004). Since the value of ΔH^0observed in the system is lower than 40 kJ mol^{-1}, the adsorption of V(V) by chemisorption mechanism is ruled out. The positive value of ΔS^0 shows the increased randomness at the solid/ solution interface during the adsorption of vanadium(V).

Linear plots of *t/q vs t* corresponding to the second order kinetic model were obtained. The calculated values of q_e agree with the experimental data. The correlation coefficients are greater than 0.99. This shows that the adsorption follows second-order kinetic model at different temperatures used in this study. Table 2 shows that the rate constant k_2 increased on increasing the temperature from 35 to 60°C.

Bangham's equation was used to evaluate whether the adsorption is pore-diffusion controlled.

$$\log\{\log[C_0/(C_0 - qM)]\} = \log(K_0 M/2.303V) + p\log t \quad (23)$$

where C_0 is initial concentration (mmol dm^{-3}), V is volume of the solution (cm^3), M is weight of the adsorbent used per liter of solution (g dm^{-3}), q is amount of adsorbate retained at time 't' (mmol g^{-1}) and p, K_0 are constants (Bhatnagar and Jain, 2005). Plots of $\log\{\log[C_0/(C_0-q_M)]\}$ *vs* $\log t$ (Fig. 8) were found to be linear for different concentrations at 35°C and 60°C, which confirms that the adsorption is pore-diffusion-controlled.

Effect of pH

The initial concentration of 20, 40, 60 and 80 mg dm^{-3} of V(V) and 200 mg/50 cm^3 of adsorbent dose were used to examine the pH effect (Fig. 9(A)). Maximum removal of V(V) occurred in the pH range 4.0 to 9.0. At pH < 4.0 and pH > 9.0 the removal was lower. According to Baes and Mesmer(1976), V(V) exists as 12 different soluble species depending on pH. They include cationic VO_2^+, neutral $VO(OH)_3$ and anionic species $V_{10}O_{26}(OH)^{3-}$, $V_{10}O_{27}(OH)^{5-}$, $V_{10}O_{28}^{6-}$ and other mono or poly vanadate species $VO_2(OH)_2^-$, $VO_3(OH)^{2-}$, VO_4^{3-}, $V_2O_6(OH)^{3-}$, $V_2O_7^{4-}$, $V_3O_9^{3-}$ and $V_4O_{12}^{4-}$. According to Blackmore et al. (1996), at pH >3.5 the dominant species is VO_3^-. Lower removal at <4.0 is due to the competition of Cl^- ions (from HCl added externally to adjust the pH) with V(V) for the adsorbent sites (also see foreign ion effect—Fig. 10). Also, adsorption of VO_2^+ species at pH < 4.0 is not favored, due to electrostatic repulsion by the positively charged adsorbent surface ($pH_{zpc} = 3.2$). At pH > 9.0, the decrease in adsorption is due to the competition of OH^- ions with the vanadate species. Also, at pH > 9.0 electrostatic repulsion occurs between the negatively charged adsorbent surface and anionic vanadate species, which hinder the adsorption of vanadate. Vanadate can be removed from the solution by the $ZnCl_2$ activated carbon by the following ion exchange mechanism (Aoki and Munemori, 1982):

Second order reaction can be represented as:

$$-\mathrm{COH} + \mathrm{VO_3^-} \rightarrow -\mathrm{C(VO_3)} + \mathrm{OH^-} \quad (24)$$

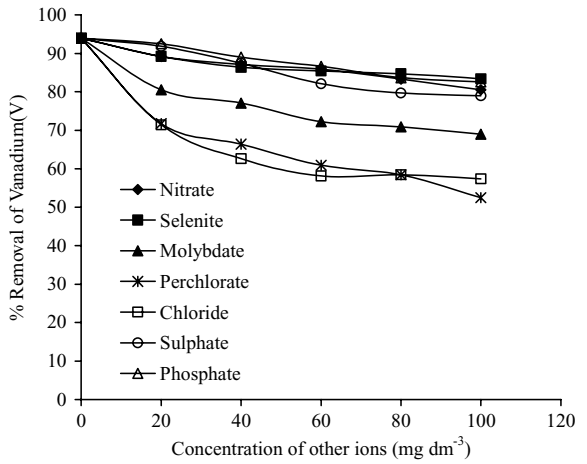

Fig. 10 Effect of different concentration of foreign ions on removal of V(V)

where ─COH represents one mole of reactive surface hydroxyls groups present in the carbon surface. With increase in pH from 9.0 to 11.0, the degree of protonation of carbon surfaces decreased gradually and hence removal was lowered by electrostatic repulsion. This is also evidenced by the experimentally observed increase in the final pH after adsorption with increase in the V(V) concentration in the initial pH range 2.0–11.0 with respect to the blank (in the absence of V(V)) (Figure not shown) (Eq. (24)). When the adsorbent is highly negatively charged (at high basic pH), adsorption is not favorable due to electrostatic repulsion between the negatively charged adsorbent surface and the anion.

Desorption studies

To make the adsorption process more economical, it is necessary to regenerate the spent carbon and V(V). Desorption was higher at pH 2.0 (30–50%) and pH 12.0 (75–90%) for different concentrations of V(V) used in this study. This is due to the release of vanadate by the Cl^- added in the form of HCl at pH < 4.0 and OH^- added at pH > 9.0. In the pH range 3.0 to 10.0 desorption was 5 to 25% for all the concentrations of V(V) studied (Fig. 9(B)). Desorption increased with increase in pH due to the increased concentration of OH^-. Effect of pH and desorption studies show that ion exchange mechanism is operative in the adsorption process. Almost complete desorption of V(V) from V(V)-laden adsorbent at pH 12.0 confirms the ion exchange mechanism (Eq. (24)). In this respect, the chemisorption mechanism given by Elovich kinetic model for the adsorption of V(V) onto $ZnCl_2$ activated coir pith carbon is not in agreement with the results of the free energy value of D-R isotherm, ΔH value, pH effect and desorption studies. It appears that the Elovich kinetic model may not represent the adsorption data.

Effect of foreign ions

Systematic examination and quantitative information on the relative competition for adsorption onto activated carbon among these anions with different binding affinities are rather scarce. Adsorption of vanadium was decreased by the addition of foreign anions–chloride, sulphate, phosphate, nitrate, selenite, molybdate and perchlorate (Fig. 10). Partitt (1978) reported that anion adsorption by soil decreased in the order $H_2PO_4^- > HAsO_4^- > HSeO_3^- = MoO_4^{2-} > SO_4^{2-} > Cl^- > NO_3^-$. In the present work other anions decreased vanadium removal in the order: $ClO_4^- > Cl^- > MoO_4^{2-} > SO_4^{2-} = PO_4^{3-} = SeO_3^{2-} = NO_3^-$.

Tests with synthetic ground water

(a) *Effect of pH*

Effect of pH on the adsorption of V(V) from simulated ground water is similar to pure V(V) solutions for the concentrations of 20 and 40 mg dm^{-3} and an adsorbent dose of 200 mg/50 cm^{-3}. Maximum removal of 75 and 70%, respectively, was observed between pH 3.0 and 7.0, for the concentrations 20 and 40 mg dm^{-3} in the ground water compared to 94 and 85% in pure V(V) solutions. The decrease in per cent removal of V(V) in ground water compared to pure V(V) solutions is attributed to the presence of other competing anions like chloride, sulfate, phosphate and nitrate in the ground water.

(b) *Effect of adsorbent dose*

Effect of adsorbent dose on adsorption of V(V) from the ground water is similar to the pure V(V) solutions for V(V) concentrations of 20 and 40 mg dm^{-3} and pH 4.0. Quantitative removal was observed at an adsorbent dose of 400 and 450 mg/50 cm^3 for the V(V) concentrations of 20 and 40 mg dm^{-3}, respectively, in the ground water compared to 250 and 350 mg/50 cm^3 in pure V(V) solutions. Higher adsorbent doses

were required for the ground water due to the presence of other competing anions like chloride, sulfate, phosphate and nitrate in the ground water.

Conclusions

This study shows that the $ZnCl_2$ activated carbon developed from agricultural waste, coir pith, is an effective adsorbent for the removal of vanadium(V) from aqueous solution. Equilibrium adsorption data better fit into Freundlich isotherm. Adsorption of vanadium(V) follows second order **and** Bangham's kinetic models. Langmuir adsorption capacity was found to be 24.9 mg g^{-1}. Adsorption was found to be maximum in the pH range 4.0 to 9.0. Increase in temperature increased the removal. The positive values of ΔH^0 confirm the endothermic nature of adsorption. pH effects and desorption studies show that ion exchange is the major mechanism in the adsorption process. Addition of different concentrations of perchlorate, chloride, molybdate and sulfate reduced the removal of vanadium, whereas phosphate, selenite and nitrate hardly influenced the removal. Tests with synthetic ground water shows that the per cent removal of V(V) anion by $ZnCl_2$ activated carbon is lower compared to pure V(V) solutions due to the presence of other competing anions.

Acknowledgment Authors are grateful to Dr. P. Weidler, Institute of Technical Chemistry, Forschungszentrum Karlsruhe, Germany for the analysis of porous properties of the carbon and Professor. Dr. T.F. Lin, National Cheng Kung University, Taiwan for the studies of SEM.

References

Abbas, A. and B.E. Conway, "Investigation of Removal of Cr(VI), MO(VI), W(VI), V(IV) and V(V) Oxyions from Industrial Wastewaters by Adsorption and Electrosorption at High-area Carbon Cloth," *J. Colloid Interf. Sci.*, **251**, 248–55 (2002).

Alkan, M., O. Demirbas, S. Celikcapa and M. Dogan, "Sorption of Acid Red 57 from Aqueous Solution Anto Sepiolite," *J. Hazard Mater.*, **B116**, 135–145 (2004).

Annual Book of ASTM Standards, Section 15, "General Products," in *Chemical Specialities and End Use Products—Activated Carbon*, ASTM International, West Conshohocken, PA, USA, Vol. 15.01 (1999).

Aoki, T. and M. Munemori, "Recovery of Cr(VI) from Wastewaters with Iron(III) Hydroxide, I. Adsorption Mechanism of Chromium(VI) on Iron(III) Hydroxide," *Water Res.*, **16**, 793–796 (1982).

APHA, *Standard Methods for the Examination of Water and Wastewater*, 18th edn. American Public Health Association, Washington, DC pp. 330–331 (1992).

Bellamy, L.J., *The Infrared Spectra of Complex Molecules*, 3rd edn. Chapman and Hall, London, Vol. 1, p. 368 (1975).

Bhargava, D.S. and S.B. Sheldarkar, "Use of TNSAC in Phosphate Adsorption Studies and Relationships, Literature, Experimental Methodology, Justification and Effects of Process Variables," *Water Res.*, **27**, 303–12 (1993).

Bhatnagar, A. and A.K. Jain, "A Comparative Adsorption Study with Different Industrial Wastes as Adsorbents for the Removal of Cationic Dyes from Water," *J. Colloid Interf. Sci.*, **281**, 49–55 (2005).

Blackmore, D.P.T., J. Ellis, and P.J. Riley, "Treatment of a Vanadium-Containing Effluent by Adsorption/Co precipitation with Iron Oxyhydroxide," *Water Res.*, **30**, 2512–2516 (1996).

Bureau of Indian Standards, *Discharge Limits of the Effluents*, IS 2490: 1981, New Delhi, 1981.

Cater, D.E. and F. Quintus, "Chemical Toxicology, Part II. Metal Toxicity," *J. Chem. Educ.*, **56**, 490–495 (1979).

Cheung, C.W., J.F. Porter, and G. McKay, "Sorption Kinetics for the Removal of Copper and Zinc from Effluents using Bone char", *Sep. Purif. Technol.*, **19**, 55–64 (2000).

Choy, K.K.H., G. McKay and J.F. Porter, "Sorption of Acid Dyes from Effluents Using Activated Carbon," *Resour. Conserv. Recy.*, **27**, 57–71 (1999).

Freundlich, H., "Uber Die Adsorption in Losungen," *Z. Phys. Chem.*, **57**, 387–470 (1906).

Gopal, M. and R.A. Gupta, "Coir Waste for a Scientific Cause," *Indian Coconut J.*, **31**,13–16 (2001).

Guzman, J., I. Saucedo, R. Navarro, J. Revilla, and E. Guibal, "Vanadium Interactions with Chitosan: Influence of Polymer Protonation and Metal Speciation," *Langmuir*, **18**, 1567–1573 (2002).

Hall, K.R., L.C. Eagleton, A. Acrivos, and T. Vermeulen, "Pore and Solid Diffusion Kinetics Infixed Bed Adsorption under Constant Pattern Conditions," *Ind. Eng. Chem. Fund.*, **5**, 212–223 (1966).

Ho, Y.S. and G. McKay, "Sorption of Dye from Aqueous Solution by Peat," *Chem. Eng. J.*, **70**, 115–124 (1998).

Jansson-Charrier, M., E. Guibal, J. Roussy, B. Delanghe, and P. Le cloirec, "Vanadium(IV) Sorption by Chitosan: Kinetics and Equilibrium," *Water Res.*, **30**, 465–475 (1996).

Jiang, Z., Y. Liu, X. Sun, F. Tian, F. Sun, C. Liang, W. You, C. Han, and C. Li, "Activated Carbons Chemically Modified by Concentrated H_2SO_4 for the Adsorption of the Pollutants from Wastewater and the Dibenzothiphene from Fuel Oils. *Langmuir*, **19**, 731–736 (2003).

Kabata-Pendias, A. and H. Pendias, *Biochemistry of Trace Elements*, PWN, Warsaw, Poland, 1993.

Kabata-Pendias, A. and H. Pendias, *Rare Elements in Biological Environment*, Geological Publication, Warsaw, Poland, 1979.

Kunz, R.G., J.F. Giannelli, and H.D. Stensel, "Vanadium Removal from Industrial Wastewaters," *J. Water Pollut. Con. F.*, **48**, 762–70 (1976).

Lagergren, S., "Zur Theorie Der Sogenannten Adsorption Geloester Stoffe," *Kungliga Svenska Vetenskapsakadomiens Handlinger.*, **24**, 1–39 (1898).

Laidler, K.J. and J.H. Meiser, *Physical Chemistry*, Houghton Mittin, New York, 1999.

Langmuir, I., "The Adsorption of Gases on Plane Surface of Glass, Mica and Platinum," *J. Am. Chem. Soc.*, **40**, 1361 (1918).

Laszlo, K. and A. Szucs, "Surface Characterization of Polyethyleneterephthalate (PET) based Activated Carbon and the Effect of pH on its Adsorption Capacity from Aqueous Phenol and 2,3,4-trichlorophenol Solutions", *Carbon*, **39**, 1945–1953 (2001).

Mahmut, O., "Equilibrium and Kinetic Modeling of Adsorption of Phosphorous on Calcined Alunite," *Adsorption*, **9**, 125–132 (2003).

Namasivayam, C. and D. Kavitha, "Adsorptive Removal of 2-Chlorophenol by Low-Cost Coir Pith Carbon," *J. Hazard. Mater.*, **98**, 257–274 (2003).

Namasivayam, C. and D. Sangeetha, "Equilibrium and Kinetic Studies of Adsorption of Phosphate onto $ZnCl_2$ Activated Coir Pith Carbon," *J. Colloid Interf. Sci.*, **280**, 359–365 (2004).

Ozcan, A.S., B. Erdem, and A. Ozcan, "Adsorption of Acid blue 913 from Aqueous Solutions onto BTMA-bentonite", *Colloid Surface A,* **266**, 73–81 (2005).

Partitt, R.L., "Anion Adsorption by Soils and Soil Materials," *Advances in Agronomy,* **30**, 1–50 (1978).

Prange, A. and K. Kremling, "Distribution of Dissolved Molybdenum, Uranium and Vanadium in Baltic Sea Waters," *Mar. Chem*., **16**, 259–274 (1985).

Sabio, M., and F.R. Reinoso, "Role of Chemical Activation in the Development and Carbon Porosity," *Colloid Surfaces A*, **241**, 15–25 (2004).

Smisek, M., and S. Cerney, *Activated Carbon, Manufacture, Properties and Applications*, Elsevier, New York, pp. 10–32 1970.

Sparks, D.L., "Kinetics of Sorption/Release Reactions at the Soil Mineral/Water Interface," In D.L. Sparks (ed.), *Soil Physical Chemistry*, 2nd edition, CRC Press, Boca Raton, FL, pp. 135–191, (1999).

Vega, E.D., J.C. Pedregosa, G.E. Narda, and P.J. Morando, "Removal of Oxovanadium(IV) from Aqueous Solutions by Using Commercial Crystalline Calcium Hydroxyapatite," *Water. Res*., **37**, 1776–1782 (2003).

Vinodhini, S., V.S. Gnanambal, and S.N. Padmadevi, "Efficacy of Degraded Coir Pith for the Growth of Medicinal Plants," *Indian Coconut. J*. **35**, 16-1-7 (2005).

Wu, F.C., R.L. Tseng, and R.S. Juang, "Preparation of Highly Microporous Carbons From Fir Wood by KOH Activation for Adsorption of Dyes and Phenols from Water," *Sep. Purif. Technol.* **47**, 10–19 (2005).

Zagulski, I., L. Pawlowski, and A. Cichocki, "Physicochemical Methods for Water and Wastewater Treatment," In L. Pawlowski L, (Ed.), *Proceedings of the Second International Conference*, Lublin 1979. Pergamon Press, Oxford, UK, (1980).

Zeng, L., X. Li, and J. Liu, "Adsorptive Removal of Phosphate from Aqueous Solutions Using Iron Oxide Tailings," *Water Res*., **38**, 1318–1326 (2004).